

Article

## Two-Photon Collective Atomic Recoil Lasing

James A. McKelvie <sup>†</sup> and Gordon R.M. Robb <sup>†,\*</sup>

Department of Physics & SUPA, University of Strathclyde, John Anderson Building, 107 Rottenrow, Glasgow G4 0NG, UK

<sup>†</sup> These authors contributed equally to this work.

\* Author to whom correspondence should be addressed; E-Mail: g.r.m.robb@strath.ac.uk;  
Tel.: +44-0141-548-3358; Fax: +44-0141-548-2891.

Academic Editors: Jonathan Goldwin and Duncan O'Dell

Received: 4 September 2015 / Accepted: 30 October 2015 / Published: 20 November 2015

---

**Abstract:** We present a theoretical study of the interaction between light and a cold gas of three-level, ladder configuration atoms close to two-photon resonance. In particular, we investigate the existence of collective atomic recoil lasing (CARL) instabilities in different regimes of internal atomic excitation and compare to previous studies of the CARL instability involving two-level atoms. In the case of two-level atoms, the CARL instability is quenched at high pump rates with significant atomic excitation by saturation of the (one-photon) coherence, which produces the optical forces responsible for the instability and rapid heating due to high spontaneous emission rates. We show that in the two-photon CARL scheme studied here involving three-level atoms, CARL instabilities can survive at high pump rates when the atoms have significant excitation, due to the contributions to the optical forces from multiple coherences and the reduction of spontaneous emission due to transitions between the populated states being dipole forbidden. This two-photon CARL scheme may form the basis of methods to increase the effective nonlinear optical response of cold atomic gases.

**Keywords:** collective atomic recoil; instabilities; two-photon

**PACS Classifications:** 42.65.Sf, 05.65.+b, 37.10.Vz

---

## 1. Introduction

The rapid progress over recent years in the ability to cool atomic gases down to temperatures of a fraction of a degree Kelvin has stimulated intense interest in fundamental aspects and applications of the interaction of light with cold and ultracold matter.

In contrast to matter-light interactions involving “hot” atomic gases or vapours, in cold atomic media, the centre-of-mass motion produced by optical forces can have a sufficiently long coherence time such that new regimes of collective behaviour can result. In this paper, we will use the term collective atomic recoil lasing (CARL) as a general label for collective instabilities that involve simultaneous growth of optical fields and atomic density modulations with periods on the scale of the optical wavelength, although it should be noted that the literature on this topic contains a number of other names for related effects, including, e.g., recoil-induced resonance, superradiant Rayleigh scattering (SRS) and optomechanics. Since the initial theoretical studies of CARL [1,2], numerous theoretical and experimental studies have been performed on related phenomena involving optical forces and cold atoms, e.g., instabilities involving self-organisation [3–23], collective cooling [24–26], optomechanical transverse pattern formation [27–32] and quantum simulation [33–35]. Experiments have involved a variety of atomic media, e.g., both thermal [8–11] and degenerate gases [3,7,12,17,20,23,33–35], and a diverse range of configurations, including optical cavities consisting of multiple mirrors [8,9,11,20,23,33–36], single mirror feedback [31] and mirrorless configurations [3,7,10,12,18,19].

Recently, there has also been interest in enhancing the nonlinear optical response of atomic gases to realise nonlinear effects at low light levels, ultimately at intensities comparable to that of single photons. It has been proposed and demonstrated that CARL-like induced bunching of atoms could play a role in providing this nonlinearity enhancement [18,19]. It is therefore timely to consider nonlinear optical interactions that combine quantum electronic nonlinearities associated with internal atomic excitation and optomechanical CARL-like behaviour. In most previous theoretical treatments of CARL, the atoms were considered to have two internal energy states, and in most cases, the population of the excited energy state was assumed to be negligible, with the atom responding to the incident optical field as a classical dipole. Increasing the level of atomic excitation in a two-level atomic system is usually undesirable for two reasons: the first is that saturating the atomic transition makes the optically-induced dipole force acting on the atoms disappear [2,37], and the second is that in two-level atoms, a significant population of the excited state leads to substantial spontaneous emission, the stochastic nature of which heats the atomic gas. For these reasons, we extend the analysis of CARL-type instabilities to a cold gas of atoms whose internal energy structure consists of three levels in a ladder configuration, as shown schematically in Figure 1, where the frequency of the light is tuned to be close to two-photon resonance, *i.e.*,  $2\omega \approx \omega_{eg}$ , where  $\omega$  is the frequency of the optical field and  $\hbar\omega_{eg}$  is the energy difference between the upper (excited) and ground state of the atom. While the atom-light coupling is inherently weaker than for two-level atoms, as it involves a two-photon resonance rather than a one-photon resonance, this system is attractive in that there are contributions to the dipole forces on the atoms originating from both one-photon and two-photon coherences, and it allows a population of atomic states between which transitions are dipole forbidden, causing spontaneous emission to be minimised and the light-atom

interaction to remain coherent. Extremely narrow linewidth dipole-forbidden transitions in cold gases of Sr and Yb have recently been proposed as the basis for the next generation of optical atomic clocks [38,39].

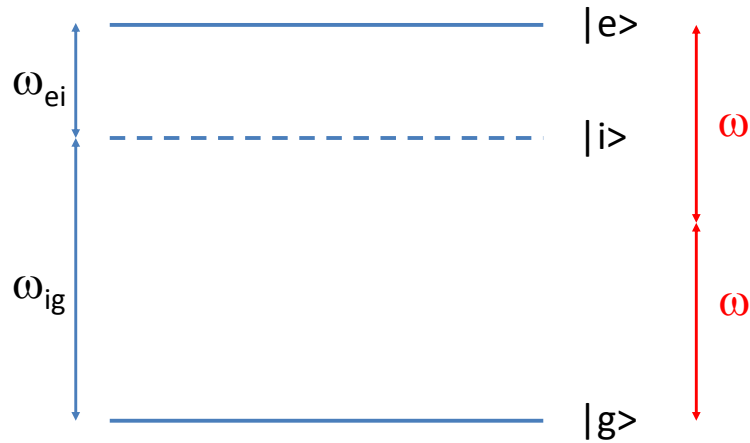


**Figure 1.** Schematic diagram of the atomic energy level structure in the two-photon model.

## 2. Model

We consider the case where the atomic gas is enclosed within a unidirectional ring cavity, as shown schematically in Figure 2. Two optical fields, a strong pump, assumed to be constant, and a weak probe, interact with a cold, collisionless atomic gas. The probe circulates in a high finesse cavity and evolves in time. It is assumed that the atomic cloud is a classical collisionless gas and that the optical fields are classical, frequency degenerate with angular frequency,  $\omega$ , and approximately counter-propagating where they interact with the atoms.

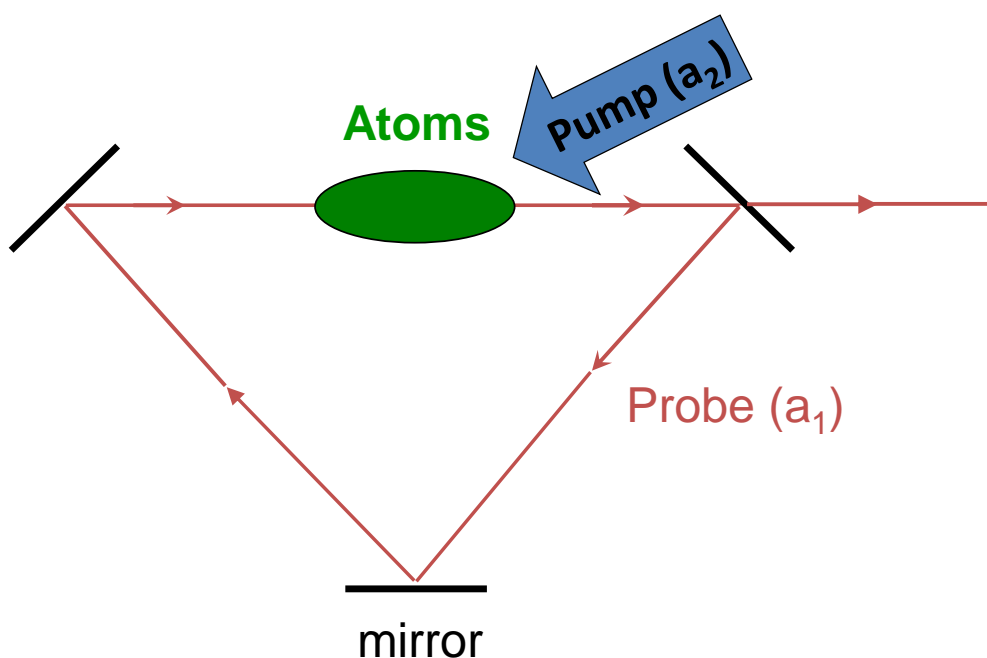


**Figure 2.** Schematic diagram of the collective atomic recoil lasing (CARL) configuration.

The model which describes the evolution of the coupled system of light and atoms consists of three main parts: the internal atomic dynamics of the atoms, the centre-of-mass motion of the atoms and the evolution of the optical field in the cavity. Here we present an outline derivation of our working equations.

### 2.1. The Three-Level Atom

We consider the case of two counter-propagating, frequency degenerate fields interacting with a three-level atom consisting of a ground state ( $|g\rangle$ ), an intermediate state ( $|i\rangle$ ) and an excited state ( $|e\rangle$ ), as shown in Figure 1. It is assumed that transitions between the ground and excited states are dipole forbidden ( $\mu_{eg} = 0$ ), but that transitions between  $|i\rangle \leftrightarrow |g\rangle$  and  $|e\rangle \leftrightarrow |i\rangle$  are dipole allowed ( $\mu_{ei} \neq 0$ ,  $\mu_{ig} \neq 0$ ). Consequently, we can write the dipole moment of each atom as:

$$\mathbf{d} = (\mu_{ig}\rho_{ig} + \mu_{ei}\rho_{ei} + c.c.) \tag{1}$$

as  $\mu_{jk} = \mu_{kj}$  and  $\rho_{jk} = \rho_{kj}^*$ . For simplicity, we assume that  $\mathbf{E} = E\hat{e}$ ,  $\mu_{ig} = \mu_{ig}\hat{e}$  and  $\mu_{ei} = \mu_{ei}\hat{e}$ , so that the Bloch equations describing the evolution of the density matrix elements  $\rho_{j,k}$  ( $j, k = g, i, e$ ) are:

$$\frac{d\rho_{gg}}{dt} = -\gamma_{gg}\rho_{gg} + i\frac{\mu_{ig}E}{\hbar}(\rho_{ig} - c.c.) \tag{2}$$

$$\frac{d\rho_{ee}}{dt} = -\gamma_{ee}\rho_{ee} - i\frac{\mu_{ig}E}{\hbar}(\rho_{ei} - c.c.) \tag{3}$$

$$\frac{d\rho_{ii}}{dt} = -\gamma_{ii}\rho_{ii} - i\frac{E}{\hbar}(\mu_{ig}\rho_{ig} - \mu_{ei}\rho_{ei} - c.c.) \tag{4}$$

$$\frac{d\rho_{ig}}{dt} = -(\gamma_{ig} + i\omega_{ig})\rho_{ig} + i\frac{E}{\hbar}(\mu_{ig}\rho_{gg} + \mu_{ei}\rho_{eg} - \mu_{ig}\rho_{ii}) \tag{5}$$

$$\frac{d\rho_{ei}}{dt} = -(\gamma_{ei} + i\omega_{ei})\rho_{ei} + i\frac{E}{\hbar}(\mu_{ei}\rho_{ii} - \mu_{ig}\rho_{eg} - \mu_{ei}\rho_{ee}) \tag{6}$$

$$\frac{d\rho_{eg}}{dt} = -(\gamma_{eg} + i\omega_{eg})\rho_{eg} + i\frac{E}{\hbar}(\mu_{ei}\rho_{ig} - \mu_{ig}\rho_{ei}) \tag{7}$$

### 2.2. The Two-Photon Approximation

We now assume that the intermediate energy level  $|i\rangle$  is sufficiently detuned from resonance with the optical fields such that its population is negligible, *i.e.*,  $\rho_{ii} = 0$ . We also assume that we have a closed system, *i.e.*,  $\gamma_{gg} = 0$  and  $\rho_{gg} + \rho_{ee} = 1$ . Making the change of variables:

$$\begin{aligned} \rho_{eg} &= s_{eg}e^{-2i\omega t} \\ \rho_{ig} &= s_{ig}e^{-i\omega t} \\ \rho_{ei} &= s_{ei}e^{-i\omega t} \\ E(z, t) &= (a_1e^{i(kz-\omega t)} + a_2e^{-i(kz+\omega t)} + c.c.) \end{aligned} \tag{8}$$

then the equations for the coherences  $\rho_{ig}$ ,  $\rho_{ei}$  and  $\rho_{eg}$ , Equations (5) and (6) reduce to:

$$\frac{ds_{ig}}{dt} = (-\gamma_{ig} + i\Delta_{ig}) s_{ig} + \frac{i}{\hbar} (\mu_{ig}\rho_{gg}(a_1e^{ikz} + a_2e^{-ikz}) + \mu_{ei}s_{eg}(a_1^*e^{-ikz} + a_2^*e^{ikz})) \quad (9)$$

$$\frac{ds_{ei}}{dt} = (-\gamma_{ei} + i\Delta_{ei}) s_{ei} - \frac{i}{\hbar} (\mu_{ig}s_{eg}(a_1^*e^{-ikz} + a_2^*e^{ikz}) + \mu_{ei}\rho_{ee}(a_1e^{ikz} + a_2e^{-ikz})) \quad (10)$$

$$\frac{ds_{eg}}{dt} = (-\gamma_{eg} + i\Delta_{eg}) s_{eg} + \frac{i}{\hbar} (\mu_{ei}s_{ig} - \mu_{ig}s_{ei}) (a_1e^{ikz} + a_2e^{-ikz}) \quad (11)$$

where  $\Delta_{ig} = \omega - \omega_{ig}$ ,  $\Delta_{ei} = \omega - \omega_{ei}$ ,  $\Delta_{eg} = 2\omega - \omega_{eg}$ ,  $p_j$  is the atomic momentum and  $m$  is the atomic mass. It is possible to adiabatically eliminate  $s_{ig}$  and  $s_{ei}$ , so that Equations (9) and (10) give:

$$s_{ig} \approx -\frac{1}{\hbar\Delta_{ig}} (\mu_{ig}\rho_{gg}(a_1e^{ikz} + a_2e^{-ikz}) + \mu_{ei}s_{eg}(a_1^*e^{-ikz} + a_2^*e^{ikz})) \quad (12)$$

$$s_{ei} \approx +\frac{1}{\hbar\Delta_{ei}} (\mu_{ig}s_{eg}(a_1^*e^{-ikz} + a_2^*e^{ikz}) + \mu_{ei}\rho_{ee}(a_1e^{ikz} + a_2e^{-ikz})) \quad (13)$$

Note that  $\Delta_{ig} + \Delta_{ei} = \Delta_{eg}$ , so close to two-photon resonance, where  $|\Delta_{eg}| \ll |\Delta_{ei}|, |\Delta_{ig}|$ , then  $\Delta_{ei} \approx -\Delta_{ig}$ , and Equation (13) becomes:

$$s_{ei} \approx -\frac{1}{\hbar\Delta_{ig}} (\mu_{ig}s_{eg}(a_1^*e^{-ikz} + a_2^*e^{ikz}) + \mu_{ei}\rho_{ee}(a_1e^{ikz} + a_2e^{-ikz})) \quad (14)$$

Substituting Equations (12) and (14) in Equations (2), (3) and (11) gives an effective two-level description in terms of quantities involving levels  $|e\rangle$  and  $|g\rangle$  only:

$$\frac{ds}{dt} = (-\gamma_{eg} + i\Delta'_{eg}) s - 2i\frac{\mu_{ig}\mu_{ei}}{\hbar^2\Delta_{ig}} (a_1^2e^{2ikz} + 2a_1a_2 + a_2^2e^{-2ikz}) D \quad (15)$$

$$\frac{dD}{dt} = -\gamma_{ee} \left( D - \frac{1}{2} \right) + i\frac{\mu_{ig}\mu_{ei}}{\hbar^2\Delta_{ig}} [(a_1^2e^{2ikz} + 2a_1a_2 + a_2^2e^{-2ikz}) s^* - c.c.] \quad (16)$$

where we have defined  $s \equiv s_{eg}$ ,  $D = \frac{\rho_{gg} - \rho_{ee}}{2}$  as two-photon coherence and population difference variables, respectively, and:

$$\Delta'_{eg} = \Delta_{eg} + \frac{\mu_{ig}^2 - \mu_{ei}^2}{\hbar^2\Delta_{ig}} (|a_1|^2 + |a_2|^2 + a_1a_2^*e^{2ikz} + a_1^*a_2e^{-2ikz})$$

which demonstrates the ACStark shift. In what follows, we assume  $\mu_{ig} = \mu_{ei} = \mu$ , so that  $\Delta'_{eg} = \Delta_{eg}$ , *i.e.*, the position- and intensity-dependent AC Stark shift is neglected.

### 2.3. Atomic Motion

The force on each atom along the cavity axis ( $z$ ) is given by:

$$F_z = \mathbf{d} \cdot \frac{\partial \mathbf{E}}{\partial z}$$

so:

$$F_z = \mu (s_{ig}e^{-i\omega t} + s_{ei}e^{-i\omega t} + c.c.) (ika_1e^{i(kz-\omega t)} - ik a_2e^{-i(kz+\omega t)} + c.c.) \quad (17)$$

Substituting for  $s_{ig}$  and  $s_{ei}$  using Equations (12) and (14), we eventually obtain:

$$F_z = -i\frac{2k\mu^2}{\hbar\Delta_{ig}} [a_1a_2^*e^{2ikz} + (a_1^2e^{2ikz} - a_2^2e^{-2ikz}) s^* - c.c.] \quad (18)$$

### 2.4. Cavity Field Evolution

The evolution of the cavity field is determined by Maxwell’s wave equation:

$$\left(\nabla^2 - \frac{1}{c^2} \frac{\partial^2}{\partial t^2}\right) \mathbf{E} = \frac{1}{\epsilon_0 c^2} \frac{\partial^2 \mathbf{P}}{\partial t^2} \quad (19)$$

where the polarisation,  $\mathbf{P}$ , for a classical gas of point particles is:

$$\mathbf{P} = \sum_j^N \mathbf{d}_j \delta(\mathbf{r} - \mathbf{r}_j(t))$$

Using the definitions of  $\mathbf{E}$  and  $\mathbf{d}_j$  in Equation (8), Equation (1) assuming  $\frac{\partial^2 \mathbf{P}}{\partial t^2} \approx -\omega^2 \mathbf{P}$ , using the slowly-varying envelope approximation (SVEA) and averaging over an interaction volume,  $V$ , we obtain:

$$\frac{da_1(t)}{dt} = \frac{i\omega c \mu n}{2\epsilon_0 c} (\langle s_{ig} e^{-ikz} \rangle + \langle s_{ei} e^{-ikz} \rangle) \quad (20)$$

Substituting for  $s_{ig}$  and  $s_{ei}$  using Equations (12) and (14), Equation (20) becomes:

$$\frac{da_1(t)}{dt} = -i \frac{\omega n \mu^2}{2\epsilon_0 \hbar \Delta_{ig}} (a_1 + a_2 \langle e^{-2ikz} \rangle + 2a_1^* \langle s e^{-2ikz} \rangle + a_2^* \langle s \rangle) + (i\delta_c - \kappa) a_1 \quad (21)$$

where  $\kappa = \frac{cT}{L_{cav}}$  is the cavity linewidth and  $\delta_c = \omega - \omega_c$  is the detuning of the pump from the cavity resonance frequency  $\omega_c$ .

The coupled set of equations that describe our system, Equations (15), (16), (18) and (21), can be written as:

$$\frac{dz_j}{dt} = \frac{p_j}{m} \quad (22)$$

$$\frac{dp_j}{dt} = -i2\hbar k U_0 [\alpha_1 \alpha_2^* e^{2ikz_j} + (\alpha_1^2 e^{2ikz_j} - \alpha_2^2 e^{-2ikz_j}) s_j^* - c.c.] \quad (23)$$

$$\frac{ds_j}{dt} = (-\gamma_{eg} + i\Delta'_{eg}) s_j - 2iU_0 (\alpha_1^2 e^{2ikz_j} + 2\alpha_1 \alpha_2 + \alpha_2^2 e^{-2ikz_j}) D_j \quad (24)$$

$$\frac{dD_j}{dt} = -\gamma_{ee} \left(D_j - \frac{1}{2}\right) + iU_0 [(\alpha_1^2 e^{2ikz_j} + 2\alpha_1 \alpha_2 + \alpha_2^2 e^{-2ikz_j}) s_j^* - c.c.] \quad (25)$$

$$\frac{d\alpha_1(t)}{dt} = -iNU_0 (\alpha_1 + \alpha_2 \langle e^{-2ikz} \rangle + 2\alpha_1^* \langle s e^{-2ikz} \rangle + \alpha_2^* \langle s \rangle) + (i\delta_c - \kappa) \alpha_1 \quad (26)$$

where  $p = mv_z$  is the atomic momentum,  $U_0 = \frac{g^2}{\Delta_{ig}}$  is the dispersive frequency shift due to a single atom,  $g = \mu \sqrt{\frac{\omega}{2\epsilon_0 \hbar V}}$  is the single photon Rabi frequency and  $\alpha_{1,2} = a_{1,2} \sqrt{\frac{2\epsilon_0 V}{\hbar \omega}}$ , so that  $|\alpha_{1,2}|^2$  represents the number of photons in the probe (1) or the pump (2) beam.

In the following section, we will investigate features of the system behaviour, in particular the existence of CARL-like instabilities in which probe/cavity field amplification occurs simultaneously with spatial modulations in the atomic density. Of particular interest is how the character of the instability changes as the degree of atomic excitation is varied. For the purposes of illustration, we will consider the ideal case where there is no incoherent decay of the excited state population or two-photon coherence,

*i.e.*,  $\gamma_{eg} = \gamma_{ee} = 0$ . We also assume that cavity losses are negligible on the time scales considered here ( $\kappa \rightarrow 0$ ), that the distribution of atomic positions is initially uniform in space and that the temperature of the atoms is initially sufficiently cold that any thermal dephasing occurs on time scales much longer than the development of the instability ( $p_j = 0 \forall j$ ).

### 3. Two-Photon CARL with Weak and Strong Excitation

We now investigate how the CARL instability changes as the degree of the excited state population is varied. We first define a reference or “saturation” pump intensity by solving Equations (24) and (25), which describe the evolution of the two-photon coherence and population difference variables  $s, D$ . Solving for  $D$  in the limit where  $\alpha_1 = 0$ , we obtain:

$$D = \frac{1}{2} \frac{\Delta_{eg}^2}{\Delta_{eg}^2 + 4U_0^2|\alpha_2|^4} + \frac{2U_0^2|\alpha_2|^4}{\Delta_{eg}^2 + 4U_0^2|\alpha_2|^4} \cos(\sqrt{\Delta_{eg}^2 + 4U_0^2|\alpha_2|^4}t)$$

Averaging over an oscillation period, this becomes:

$$D = \frac{1}{2} \frac{\Delta_{eg}^2}{\Delta_{eg}^2 + 4U_0^2|\alpha_2|^4} \tag{27}$$

so we can define a “saturation” pump intensity as being that for which the average excited-state population,  $\rho_{ee}$ , is 1/4, *i.e.*,  $D = 1/4$ . From Equation (27), it can be seen that this occurs when the pump photon number is:

$$|\alpha_2|^2 \equiv |\alpha_2|_{\text{sat}}^2 = \left| \frac{\Delta_{eg}}{2U_0} \right| \tag{28}$$

We first consider the limit  $|\alpha_2|^2 \ll |\alpha_2|_{\text{sat}}^2$ , such that each atom is only weakly excited internally and almost all of the atomic population remains in the ground state,  $|g\rangle$ , *i.e.*,  $D \rightarrow \frac{1}{2}$  and  $s \rightarrow 0$ . In this limit, Equations (22)–(26) reduce to:

$$\frac{dz_j}{dt} = \frac{p_j}{m} \tag{29}$$

$$\frac{dp_j}{dt} = -i2\hbar kU_0 (\alpha_1 \alpha_2^* e^{2ikz_j} - c.c.) \tag{30}$$

$$\frac{d\alpha_1(t)}{dt} = -iNU_0 (\alpha_1 + \alpha_2 \langle e^{-2ikz} \rangle) + (i\delta_c - \kappa) \alpha_1 \tag{31}$$

which, when written in terms of the dimensionless variables:

$$\theta = 2kz \quad , \quad \bar{p} = \frac{2}{\rho} p \quad , \quad \bar{a} = \sqrt{\frac{2}{\rho N}} \alpha_1$$

become the CARL equations originally derived for two-level atoms [1,2] in the so-called free-electron laser (FEL) limit [37]:

$$\frac{d\theta_j}{d\tau} = \bar{p}_j \tag{32}$$

$$\frac{d\bar{p}_j}{d\tau} = -(\bar{a} e^{i\theta_j} + c.c.) \tag{33}$$

$$\frac{d\bar{a}}{d\tau} = \langle e^{-i\theta} \rangle - \bar{\kappa} \bar{a} \tag{34}$$

where  $\alpha_2 = -i|\alpha_2|$  and  $\delta_c = NU_0$  have been assumed, the dimensionless time coordinate  $\tau = \omega_r \rho t$ , the cavity decay rate  $\bar{\kappa} = \frac{\kappa}{\omega_r \rho}$ ,  $\omega_r = \frac{2\hbar k^2}{m}$  is the recoil frequency and the scaling parameter  $\rho$  is defined as:

$$\rho = \left( \frac{2NU_0^2 |\alpha_2|^4}{\omega_r^2} \right)^{1/3}$$

It has been shown in, e.g., [1,2,37] that these equations display a collective instability in which the initially homogeneous distribution of atomic positions is unstable and the resulting instability involves exponential growth of both the probe field intensity ( $|\bar{a}|^2$ ) and density modulation amplitude/spatial order parameter ( $|b| = |\langle e^{-i\theta} \rangle|$ ).

An example of the system evolution in the weak-excitation regime is shown in Figures 3, 4 and 5. Figure 3 shows the evolution of the cavity field intensity, bunching parameter and average population difference, respectively. It can be seen that an exponential growth of the cavity field intensity occurs simultaneously with the growth of the bunching parameter, indicating the development of a strong modulation in the atomic density with spatial period  $\lambda/2$ , in common with the behaviour of the CARL instability in two-level systems [1,2,37]. The development of this density modulation is clearly seen in the snapshots of the phase space  $(\theta, p)$  shown in Figure 4. In contrast to the behaviour of the atomic motion, Figure 3 and the snapshots of the atomic population distribution  $(\theta, D)$  shown in Figure 5 show that the atomic population difference does not deviate significantly from its original value, with the atomic population remaining almost entirely spatially uniform and in the ground state.

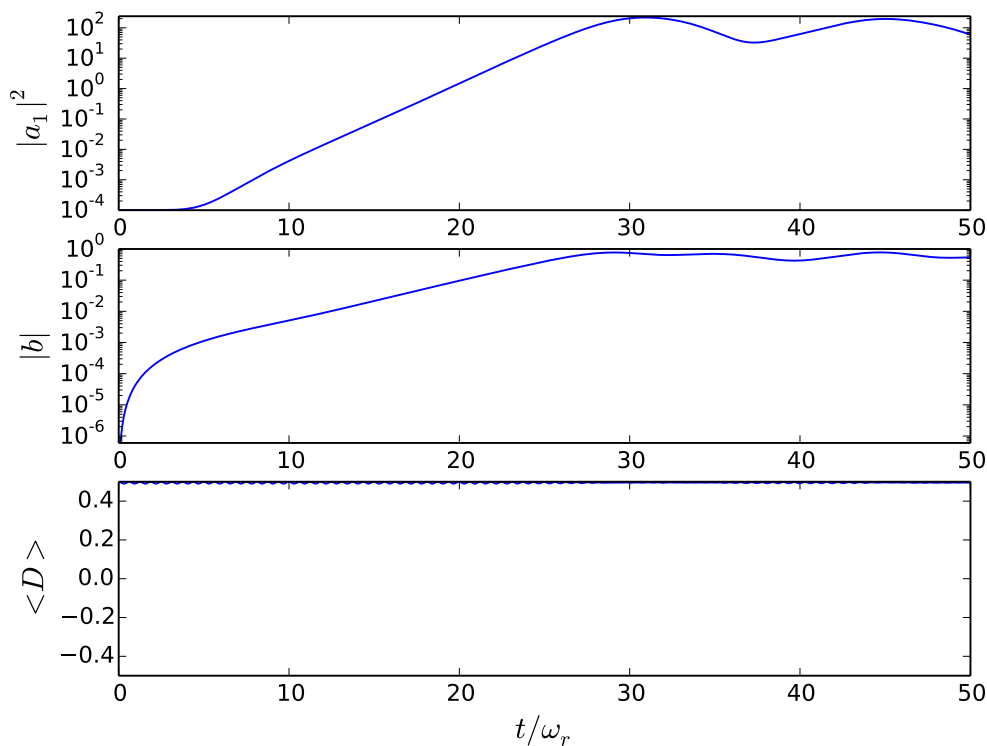


**Figure 3.** Evolution of probe photon number,  $|\alpha_1|^2$ , bunching parameter,  $|b|$ , and mean population difference,  $\langle D \rangle$ , for a case of weak excitation. The parameters used are  $U_0/\omega_r = 5 \times 10^{-5}$ ,  $\Delta_{eg} = 10$ ,  $\alpha_2 = 100$ ,  $N = 1000$ .



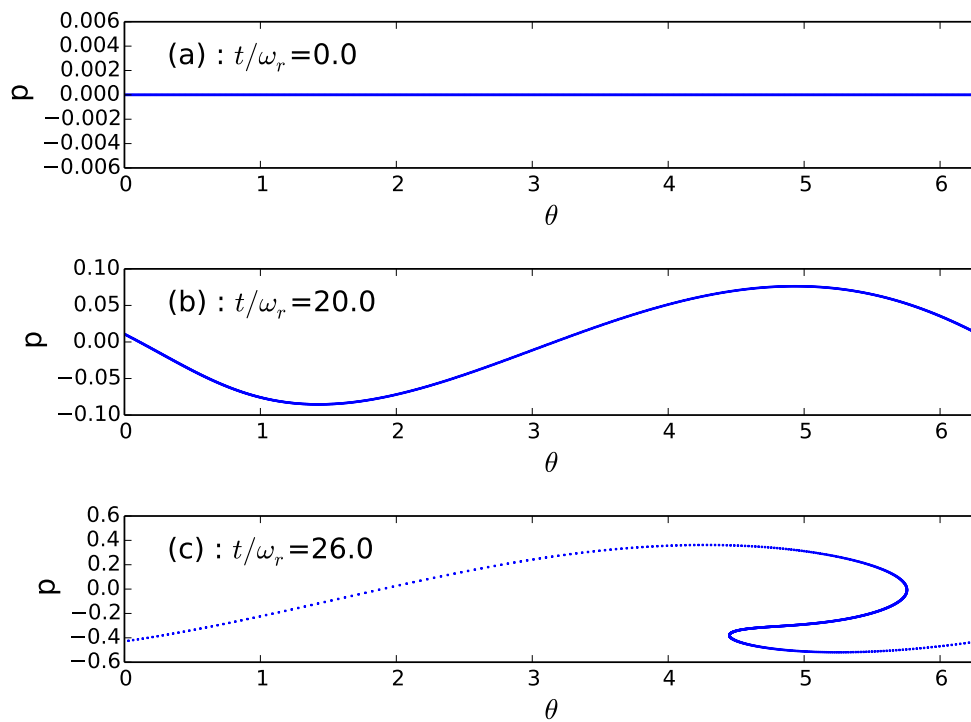


**Figure 4.** Snapshots of momentum distribution  $(\theta_j, p_j)$  for each atom  $j = 1..1000$  when (a)  $t = 0\omega_r^{-1}$ , (b)  $t = 20\omega_r^{-1}$  and (c)  $t = 26\omega_r^{-1}$  in the case of weak excitation. The parameters used are as in Figure 3.

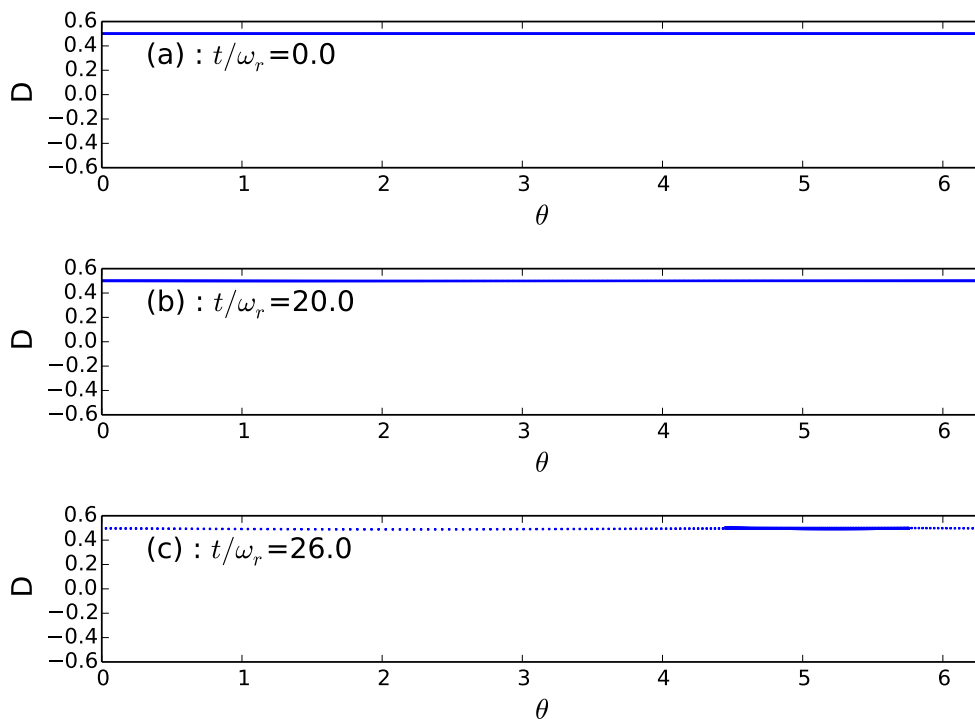


**Figure 5.** Snapshots of population difference distribution  $(\theta_j, D_j)$  for each atom  $j = 1..1000$  when (a)  $t = 0\omega_r^{-1}$ , (b)  $t = 20\omega_r^{-1}$  and (c)  $t = 26\omega_r^{-1}$  in the case of weak excitation. The parameters used are as in Figure 3.

### 4. Strong Excitation

An example of the system evolution in the strong pump limit is shown in Figures 6–8. From Figure 6, it can be seen that, again, an exponential growth of the cavity field intensity occurs simultaneously with the growth of the bunching parameter. In contrast to the weak excitation limit, Figure 6 and the snapshots of the atomic population distribution  $(\theta, D)$  shown in Figure 8 show that the atomic population difference now also undergoes significant evolution during the instability, deviating significantly from its original value of 0.5. Figure 6 shows that after rapid (two-photon) Rabi oscillations, the population difference results in a strongly periodic distribution of atomic population in addition to the strongly periodic spatial distribution of atomic positions/density. The amplitude of the population difference modulation is sufficiently large such that a significant number of atoms have  $D < 0$ , *i.e.*, their internal population is inverted. In a two-level atom, this would result in significant spontaneous emission and, consequently, heating, due to the stochastic nature of the recoil associated with spontaneous emission events, but the three-level/two-photon configuration considered here avoids this and allows significant population of the upper state while retaining the coherence of the system. It should also be noted that in two-level atoms, strong pumping and, consequently, the strong population of the upper state would result in  $D \rightarrow 0$  on average [37], and the dipole force, which bunches the atoms, would also disappear. As can be seen from Figure 6, this does not happen in the case considered here, because the dipole force contains contributions from the one-photon coherences  $\rho_{ei}, \rho_{ig}$ , which are not saturated, in addition to the two-photon coherence,  $s$ . The damping of the Rabi oscillations seen in Figure 6c occurs when the probe intensity is amplified to values comparable to that of the pump. At this point, the position  $(\theta)$  dependence of the total field driving the populations of the atoms becomes significant (see Equations (24) and (25)). Consequently, the momentum spread induced by the atomic bunching/CARL instability causes the atoms to experience different fields, which dephases their Rabi oscillations.

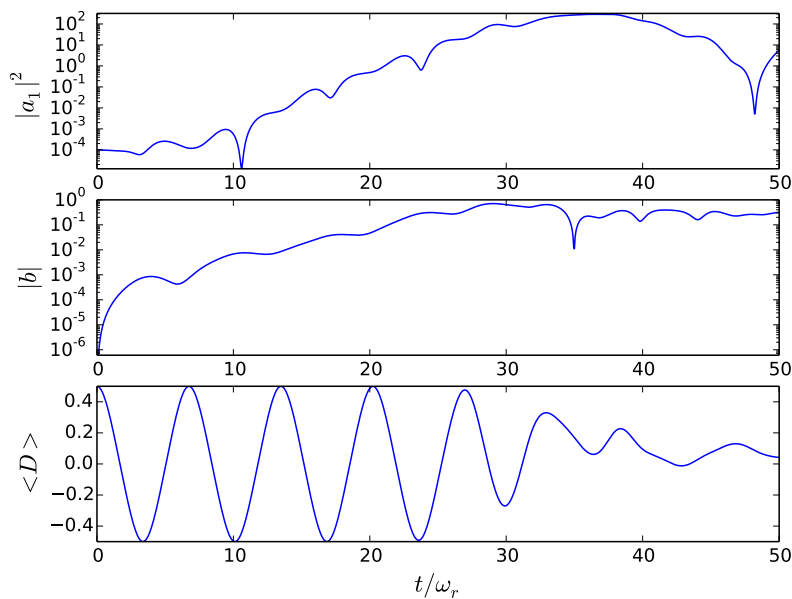


**Figure 6.** Evolution of probe photon number,  $|\alpha_1|^2$ , bunching parameter,  $|b|$ , and mean population difference,  $\langle D \rangle$ , for a case of strong excitation. The parameters used are  $U_0/\omega_r = 5 \times 10^{-5}$ ,  $\Delta_{eg} = 1$ ,  $\alpha_2 = 100$ ,  $N = 1000$ .

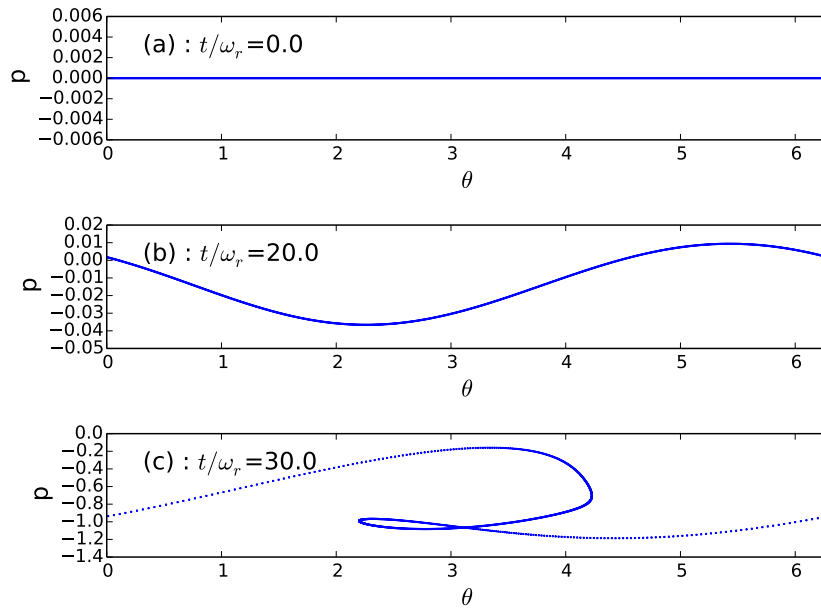


**Figure 7.** Snapshots of momentum distribution  $(\theta_j, p_j)$  for each atom  $j = 1..1000$  when (a)  $t = 0\omega_r^{-1}$ , (b)  $t = 20\omega_r^{-1}$  and (c)  $t = 30\omega_r^{-1}$  in the case of strong excitation. The parameters used are as in Figure 6.

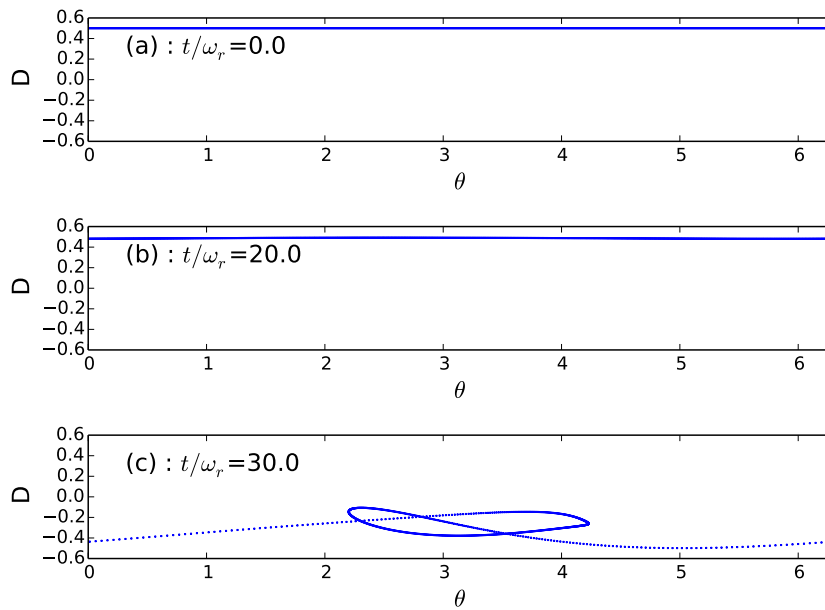


**Figure 8.** Snapshots of population difference distribution  $(\theta_j, D_j)$  for each atom  $j = 1..1000$  when (a)  $t = 0\omega_r^{-1}$ , (b)  $t = 20\omega_r^{-1}$  and (c)  $t = 30\omega_r^{-1}$  in the case of strong excitation. The parameters used are as in Figure 6.

### 5. Conclusions

We have performed a theoretical study of a CARL instability involving a cold gas of three-level atoms. In contrast to previous theoretical treatments of CARL, the atoms were considered to have three

internal energy states in a ladder configuration where transitions between the lowest and highest states are dipole forbidden. It was shown that when the population of the excited (highest) state is small, the behaviour of the system reduces to that of previous studies of CARL in two-level atomic systems. However, when the level of the atomic system is increased, the behaviour of the system diverges from that of the two-level model, as the existence of a collective instability involving strong bunching/density modulation persists in the three-level system. Even though the bunched atoms are highly excited, the rate of spontaneous emission will be small, as transitions to the ground state are dipole forbidden. While the atom-light coupling is inherently weaker in this three-level ladder scheme than for two-level atoms, as it involves a two-photon resonance rather than a one-photon resonance, this system offers advantages in that there are contributions to the dipole forces on the atoms that are not saturated and that it allows a significant population of atomic states between which transitions are dipole forbidden and spontaneous emission rates are small. Candidates for the realisation of the effects predicted here are gases of alkaline-earth-like atoms, e.g., Sr or Yb, which can be cooled and possess long-lived/metastable states due to forbidden transitions.

The coherent nature of the interaction, even in the absence of high levels of atomic excitation, suggests that such instabilities should exist not only in classical gases, but also in BECs. This offers the intriguing prospect of simultaneous, coherent control of discrete electronic and momentum states of a BEC.

### Acknowledgements

We acknowledge financial support from the EPSRC in the form of a DTG studentship.

### Author Contributions

Both authors contributed equally to this work.

### Conflicts of Interest

The authors declare no conflict of interest.

### References

1. Bonifacio, R.; de Salvo, L. Collective atomic recoil laser (CARL) optical gain without inversion by collective atomic recoil and self-bunching of two-level atoms. *Nucl. Instrum. Meth. Phys. Res. A* **1994**, *341*, 360–362.
2. Bonifacio, R.; de Salvo Souza, L.; Narducci, L.; D'Angelo, E.J. Exponential gain and self-bunching in a collective atomic recoil laser. *Phys. Rev. A* **1994**, *50*, 1716–1724.
3. Inouye, S.; Chikkatur, A.P.; Stamper-Kurn D.M.; Stenger, J.; Pritchard, D.E.; Ketterle, W. Superradiant Rayleigh scattering from a Bose-Einstein condensate. *Science* **1999**, *285*, 571–574.
4. Moore, M.G.; Meystre, P. Theory of superradiant scattering of laser light from Bose-Einstein condensates. *Phys. Rev. Lett.* **1999**, *83*, 5202–5205.
5. Gangl, M.; Ritsch, H. Cold atoms in a high-Q ring cavity. *Phys. Rev. A* **2000**, *61*, 043405.

6. Piovella, N.; Gatelli, M.; Bonifacio, R. Quantum effects in the collective light scattering by coherent atomic recoil in a Bose–Einstein condensate. *Opt. Commun.* **2001**, *194*, 167–173.
7. Schneble, D.; Torii, Y.; Boyd, M.; Streed, E.W.; Pritchard D.E.; Ketterle, W. The onset of matter–wave amplification in a superradiant Bose–Einstein condensate. *Science* **2003**, *300*, 475–478.
8. Kruse, D.; von Cube, C.; Zimmermann, C.; Courteille, Ph.W. Observation of lasing mediated by collective atomic recoil. *Phys. Rev. Lett.* **2003**, *91*, 183601.
9. Nagorny, B.; Elsässer, Th.; Hemmerich, A. Collective atomic motion in an optical lattice formed inside a high finesse cavity. *Phys. Rev. Lett.* **2003**, *91*, 153003.
10. Yoshikawa, Y.; Torii, Y.; Kuga, T. Superradiant light scattering from thermal atomic vapors. *Phys. Rev. Lett.* **2005**, *94*, 083602.
11. Von Cube, C.; Slama, S.; Kruse, D.; Zimmermann, C.; Courteille, Ph.W.; Robb, G.R.M.; Piovella, N.; Bonifacio, R. Self-Synchronization and Dissipation-Induced Threshold in Collective Atomic Recoil Lasing. *Phys. Rev. Lett.* **2004**, *93*, 083601.
12. Fallani, L.; Fort, C.; Piovella, N.; Cola, M.M.; Cataliotti, F.S.; Inguscio, M.; Bonifacio, R. Collective atomic recoil in a moving Bose–Einstein condensate: From superradiance to Bragg scattering. *Phys. Rev. A* **2005**, *71*, 033612.
13. Asboth, J.K.; Domokos, P.; Ritsch, H.; Vukics, A. Self–organization of atoms in a cavity field: Threshold, bistability, and scaling laws. *Phys. Rev. A* **2005**, *72*, 053417.
14. Nagy, D.; Asboth, J.K.; Domokos, P.; Ritsch, H. Self–organization of a laser–driven cold gas in a ring cavity. *Europhys. Lett.* **2006**, *74*, 254.
15. Slama, S.; Bux, S.; Krenz, G.; Zimmermann, C.; Courteille, Ph.W. Superradiant Rayleigh scattering and collective atomic recoil lasing in a ring cavity. *Phys. Rev. Lett.* **2007**, *98*, 053603.
16. Keeling, J.; Bhaseen, M.J.; Simons, B.D. Collective dynamics of Bose–Einstein condensates in optical cavities. *Phys. Rev. Lett.* **2010**, *105*, 043001.
17. Bux, S.; Gnahn, C.; Maier, R.A.W.; Zimmermann C.; Courteille, Ph.W. Cavity–Controlled Collective Scattering at the Recoil Limit. *Phys. Rev. Lett.* **2011**, *106*, 203601.
18. Greenberg, J.A.; Schmittberger, B.L.; Gauthier, D.J. Bunching–induced optical nonlinearity and instability in cold atoms. *Opt. Express* **2011**, *19*, 22535.
19. Schmittberger, B.L.; Gauthier, D.J. Enhancing light–atom interactions via atomic bunching. *Phys. Rev. A* **2014**, *90*, 013813.
20. Kessler, H.; Klinder, J.; Wolke, M.; Hemmerich, A. Steering matter wave superradiance with an ultranarrow–band optical cavity. *Phys. Rev. Lett.* **2014**, *113*, 070404.
21. Keeling, J.; Bhaseen, M.J.; Simons, B.D. Fermionic Superradiance in a Transversely Pumped Optical Cavity. *Phys. Rev. Lett.* **2014**, *112*, 143002 .
22. Fernández-Vidal, S.; de Chiara, G.; Larson, J.; Morigi, G. Quantum ground state of self–organized atomic crystals in optical resonators. *Phys. Rev. A* **2010**, *81*, 043407.
23. Schmidt, D.; Tomczyk, H.; Slama, S.; Zimmermann, C. Dynamical Instability of a Bose–Einstein Condensate in an Optical Ring Resonator. *Phys. Rev. Lett.* **2014**, *112*, 115302.
24. Domokos, P.; Ritsch, H. Collective cooling and self–organization of atoms in a cavity. *Phys. Rev. Lett.* **2002**, *89*, 253003.

25. Chan, H.W.; Black, A.T.; Vuletic, V. Observation of collective–emission–induced cooling of atoms in an optical cavity. *Phys. Rev. Lett.* **2003**, *90*, 63003.
26. Black, A.T.; Chan, H.W.; Vuletic, V. Observation of collective friction forces due to spatial self–organization of atoms: From Rayleigh to Bragg scattering. *Phys. Rev. Lett.* **2003**, *91*, 203001.
27. Muradyan, G.A.; Wang, Y.; Williams, W.; Saffman, M. Absolute instability and pattern formation in cold atomic vapors. *Nonlinear Guided Waves Top. Meet. Tech. Dig.* **2005**, doi:10.1364/NLGW.2005.ThB29.
28. Saffman, M.; Wang, Y. Collective focusing and modulational instability of light and cold atoms. In *Dissipative Solitons: From Optics to Biology and Medicine*; Springer: Berlin, Germany, 2008.
29. Tesio, E.; Robb, G.R.M.; Ackemann, T.; Firth, W.J.; Oppo, G.-L. Spontaneous optomechanical pattern formation in cold atoms. *Phys. Rev. A* **2012**, *86*, 031801.
30. Tesio, E.; Robb, G.R.M.; Ackemann, T.; Firth, W.J.; Oppo, G.-L. Kinetic theory for transverse optomechanical instabilities. *Phys. Rev. Lett.* **2012**, *112*, 043901.
31. Labeyrie, G.; Tesio, E.; Gomes, P.M.; Oppo, G.-L.; Firth, W.J.; Robb, G.R.M.; Arnold, A.S.; Kaiser, R.; Ackemann, T. Optomechanical self-structuring in a cold atomic gas. *Nat. Phot.* **2014**, *8*, 321–325.
32. Robb, G.R.M.; Tesio, E.; Oppo, G.-L.; Firth, W.J.; Ackemann, T.; Bonifacio, R. Quantum Threshold for Optomechanical Self-Structuring in a Bose-Einstein Condensate. *Phys. Rev. Lett.* **2015**, *114*, 173903.
33. Brennecke, F.; Ritter, S.; Donner, T.; Esslinger, T. Cavity optomechanics with a Bose–Einstein condensate. *Science* **2008**, *322*, 235–238.
34. Baumann, K.; Guerlin, C.; Brennecke, F.; Esslinger, T. Dicke quantum phase transition with a superfluid gas in an optical cavity. *Nature* **2010**, *464*, 1301–1306.
35. Botter, T.; Brooks, D.W.C.; Schreppler, S.; Brahms, N.; Stamper-Kurn, D.M. Optical readout of the quantum collective motion of an array of atomic ensembles. *Phys. Rev. Lett.* **2013**, *110*, 153001.
36. Ritsch, H.; Domokos, P.; Brennecke, F.; Esslinger, T. Cold atoms in cavity-generated dynamical optical potentials. *Rev. Mod. Phys.* **2013**, *85*, 553–601.
37. Bonifacio, R.; de Salvo, L. Analytical theory of the collective atomic recoil laser in the FEL limit. *Appl. Phys. B* **1995**, *60*, S233–S239.
38. Katori, H.; Takamoto, M.; Pal’chikov, V.G.; Ovsianikov, V.D. Ultrastable Optical Clock with Neutral Atoms in an Engineered Light Shift Trap. *Phys. Rev. Lett.* **2003**, *91*, 173005 .
39. Ludlow, A.D.; Hinkley, N.M.; Sherman, J.A.; Phillips, N.B.; Schioppo, M.; Lemke, N.D.; Beloy, K.P.; Pizzocaro, M.; Oates, C.W. An atomic clock with  $10^{-18}$  instability. *Science* **2013**, *341*, 1215–1218.